Electrical-Mechanical Dynamic Modelling and Testing of a Lightweight-Link Robot Manipulator

Frederik Foldager, Dan Thomsen, Haijie Li, Kasper Frederiksen, Anders Andersen, Xuping Zhang

Aarhus University, Department of Engineering & Aarhus School of Engineering
Inge Lehmanns Gade 10, 8000 Aarhus C, Denmark
xuzh@ase.au.dk

Abstract –This paper presents the electrical-mechanical dynamic modelling and testing of a lightweight-link robot manipulator. Mechanical dynamic modelling of lightweight robot manipulators has received extensive attention with the consideration of link flexibility. However few efforts have been paid to the electrical-mechanical dynamic modelling of lightweight-link manipulators which will provide the essential insights to control the motion and vibration of lightweight robot manipulators. In this work, the sub-model of an actuator (a DC servo motor) dynamics and the sub-model of vibration dynamics of a driven lightweight-link are established separately. Then the two sub-models are integrated to form a comprehensive electrical-mechanical dynamic model. The proposed electrical-mechanical model is applied to a single lightweight link robot manipulator. The simulations and dynamics characterization are conducted to provide insights into the control and design of lightweight link robot manipulators. A real-time testing and control system is setup, and experimental testing is performed to validate the proposed electrical-mechanical modelling and dynamic characterization analyses.

Keywords: Lightweight Robot Manipulators, Electrical-Mechanical Dynamics, Elastic Vibration, Vibration Testing, Boundary Conditions, Vibration Modes, Laplace Transform, Transfer Function

1. Introduction

It is desirable to design and construct lightweight manipulators for manufacturing and aerospace applications which require robot manipulator to be capable of moving swiftly. In contrast to the rigid manipulators, lightweight manipulators offer advantages such as higher speed, better energy efficiency, improved mobility, and higher payload-to-arm weight ratio. However, at high operational speeds, inertial forces of moving components become quite large, leading to considerable deformation in the lightweight links, and generating unwanted vibration phenomena. Hence, the flexibility of lightweight links must be taken into account in the modelling, design, and control of the robot manipulators.

In the past decades, significant progresses have been made into the dynamic modelling of manipulators or mechanisms with flexible links (Lowen and Jandrasits, 1972; Lowen and Chassapis, 1986; Shabana, 1997; Dwivedy and Eberhard, 2006; Book, 1993; Benosman and Vey, 2004). Different discretization techniques, such as the finite element method (FEM) (Erdman et al, 1972; Immam and Kraner, 1973; Nath and Ghosh, 1980; Cleghorn et al, 1981; Turic and Midha, 1984; Zhang and Yu, 2000; Usoro et al, 1986), the assumed mode method (AMM) (Book, 1984; Asada et al, 1990; Baruh and Tadikonda, 1989; Hustings and Book, 1986; Barieri and Ozguner, 1988; Bellezza et al, 1990; Low and Lau, 1995; Shabana, 1996; Zhang et al, 2007), and the lumped parameter method (LPM) (Ge et al, 1997; Tosunogle et al, 1992; Megahed and Haza, 2004; Mihai and Siamak, 2014), have been reported extensively for modelling the dynamics of flexible-link robot manipulators or mechanisms. However, few efforts have been devoted to generating an electrical-mechanical dynamic model of a flexible-link robot manipulator by including the actuation dynamics (i.e. motor dynamics). The electrical-mechanical dynamic model will provide essential insights to the control of robot motions and vibrations for achieving the satisfactory performance.

This research aims to developing an electrical-mechanical dynamic model by integrating the actuator dynamics and the vibration dynamics of a driven lightweight link, and investigating the dynamic characteristics. The electrical-mechanical model is applied to a single lightweight-link robot manipulator. Numerical simulations are performed using the developed dynamic models, and experimental testing is conducted using an in-house developed real-time testing and control system based on LabView real-time software and hardware. The simulation and testing results are analysed and compared to validate the proposed dynamic modelling of lightweight-link robot manipulators.

2. Overview of Electrical-Mechanical Modelling

For the simplicity, a single flexible-link manipulator driven by a permanent magnet DC motor is presented to illustrate the procedure and principle of electrical-mechanical modelling. As shown in Fig. 1, the physical model is divided into a DC motor and a slewing beam. Dynamic modelling is first conducted for the DC motor by defining the voltage/current as an input, and the angular velocity/position as an output. Then the slewing beam dynamic modelling is performed by defining the angular position as an input and the elastic deformation as an output. The two sub-models are finally integrated into a system dynamic model of the flexible-link manipulator.
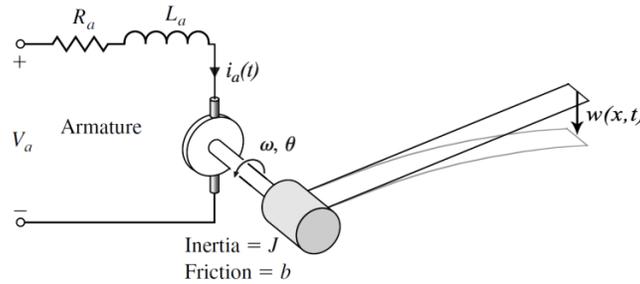
Fig. 1. Schematic diagram of a single flexible-link manipulator driven by a DC motor

3. Dynamics of a DC Motor

In this section, a dynamic model of a DC motor is established based on the working principle of a DC motor: Kirchhoff's law, electro-magnetic force, and rotor dynamics. In the model, the input is defined as voltage or current, and the output is defined as angular velocity or position.

3. 1. Open-Loop Dynamics of a DC Motor

In this work, a permanent magnet DC motor is chosen to drive the lightweight manipulator. A permanent magnet DC motor is controlled by adjusting the current or voltage of the armature because the field current is assumed as constant. Without control loops, the dynamics of a permanent magnet DC motor can be expressed using a block diagram as shown in Fig. 2 where $V_a(s)$ is the voltage input to the DC motor, $V_a'(s) = V_a(s) - V_b(s)$ the effective voltage applied to the armature, $V_b(s) = K_b\omega(s)$ the back electromotive-force voltage, K_b the electromotive-force constant, $\omega(s)$ the angular velocity output of the motor, $\theta(s)$ the angular position output of the motor, R_a the armature resistance, L_a the armature inductance, T_m the motor torque, T_L the load torque, T_d the disturbance torque, J the rotor inertia, and b is the viscous damping coefficient.

The voltage applied to the armature can be written as using Kirchhoff's equation as

$$V_a'(t) = V_a(t) - V_b(t) = R_a i_a(t) + L_a \frac{di_a(t)}{dt} \tag{1}$$

Where i_a is the armature current. Taking Laplace transform, the armature current can be written in the Laplace domain as

$$i_a(s) = \frac{V_a'(s)}{R_a + L_a s} = \frac{V_a(s) - V_b(s)}{R_a + L_a s} = \frac{V_a(s) - K_b \omega(s)}{R_a + L_a s} = \frac{V_a(s) - s K_b \theta(s)}{R_a + L_a s} \qquad (2)$$
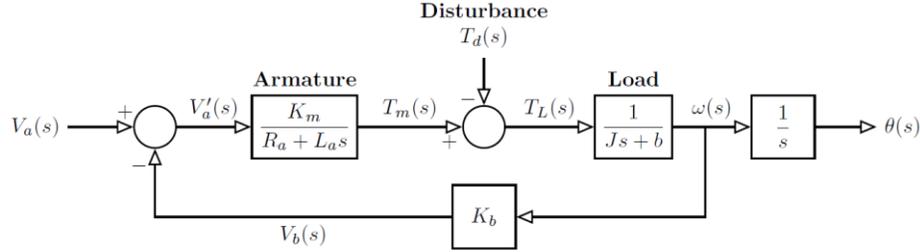
Fig. 2. Block diagram of a permanent magnet DC motor without closed-loop control

The motor torque can be calculated as $T_m(s) = K_m(s) i_a(s) = \frac{K_m V_a'(s)}{R_a + L_a s}$ as shown in Fig. 2 where K_m is the motor constant or the torque constant.

On the other hand, the rotor dynamics of the motor can be written based on the Newton's second law as

$$J \frac{d^2 \ddot{\theta}(t)}{dt^2} + b \frac{d\theta(t)}{dt} = T_L(t) = T_m(t) - T_d(t) \qquad (3)$$

Eqn. (3) can be written in the format of the transfer function in the Laplace domain as: $\frac{\theta(s)}{T_L(s)} = \frac{1}{(Js+b)s}$.

Based on the block diagram, the transfer function of the angular position to the applied voltage can be calculated as

$$G_{\theta V}(s) = \frac{\theta(s)}{V_a(s)} = \frac{K_m}{L_a J s^3 + R_a J s^2 + (R_a b + K_m K_b)s} \qquad (4)$$

Taking the inverse Laplace transform of Eqn. (4), the dynamic differential equation of the DC motor in the time domain can be written as

$$\frac{L_a J}{K_m} \frac{d^3 \theta(t)}{dt^3} + \frac{R_a J}{K_m} \frac{d^2 \theta(t)}{dt^2} + \left(\frac{R_a b}{K_m} + K_b\right) \frac{d\theta(t)}{dt} = V_a(t) \qquad (5)$$

Eqn. (5) is the 3rd order ordinary differential equation representing the open-loop dynamics of the DC motor with the input of the applied voltage $V_a(t)$ and the output of the angular position $\theta(t)$.

3. 2. Closed-loop Feedback Control Dynamics of a DC motor

To achieve precise motion and robustness against the disturbance, it is imperative to add a closed-loop feedback controller to the system. In this work, the PD position controller is added to achieve the precise angular position of the motor shaft as shown in Fig. 3. Substituting $V_a(t) = K_\omega \frac{d(\theta_d - \theta)}{dt} + K_\theta(\theta_d - \theta)$ into Eqn. (5), the dynamic equation with the PD feedback controller of the DC motor can be derived by as

$$\frac{L_a J}{K_m} \frac{d^3 \theta(t)}{dt^3} + \frac{R_a J}{K_m} \frac{d^2 \theta(t)}{dt^2} + \left(\frac{R_a b}{K_m} + K_b\right) \frac{d\theta(t)}{dt} = V_a(t) = K_\omega \frac{d(\theta_d - \theta)}{dt} + K_\theta(\theta_d - \theta) \qquad (6)$$

where θ_d is the desired angular position that is defined as the precision motion. Eqn. (6) can be reorganized as

$$\frac{L_a J}{K_m}\frac{d^3\theta(t)}{dt^3} + \frac{R_a J}{K_m}\frac{d^2\theta(t)}{dt^2} + \left(\frac{R_a b}{K_m} + K_b + K_\omega\right)\frac{d\theta(t)}{dt} + K_\theta\theta(t) = K_\omega\frac{d\theta_d}{dt} + K_\theta\theta_d \tag{7}$$

Fig. 3. Block diagram of a permanent magnet DC motor under PD feedback position control

4. Dynamics of a Slewing Flexible Beam

To model the flexibility of a slewing beam, the continuous beam can be discretized using the finite element method (FEM), the assumed mode method (AMM), and the lumped parameter method (LPM). In this work, the AMM and the LPM are employed to establish the dynamic equation of a slewing beam as shown in Fig. 1.

In the AMM, the deformation of the continuous beam is expressed as the linear superposition of the vibrations contributed from all the vibration modes, namely, $w(x,t) = \sum_{i=1}^{n}\eta_i(t)\cdot\psi_i(x)$ where $\psi_i(x)$ is the ith order modal shape function of the slewing beam, and $\eta_i(t)$ is the ith modal coordinate. The modal shape functions are calculated based on the boundary conditions. For the slewing beam driven by a DC motor, the boundary conditions are approximated by treating one end to be fixed and one end to be free. Based on the fixed-free boundary condition, the modal shape function is given as

$$\psi_i(x) = C_i[sin(\beta_i x) - sinh(\beta_i x) - \alpha_i(cos(\beta_i x) - cosh(\beta_i x))] \tag{8}$$

where $\alpha_i = \frac{sin(\beta_i l)+sinh(\beta_i l)}{cos(\beta_i l)+cosh(\beta_i l)}$, l is the length of the beam, and β_i is calculated based on the frequency equation: $cosh(\beta\cdot l)\cdot cos(\beta\cdot l) = -1$. The frequency of the ith mode can be calculated using $\omega_i = (\beta_i\cdot l)^2\cdot\sqrt{\frac{E\cdot I}{\rho\cdot A\cdot l^4}}$ where ρ is the material density, A cross-sectional area of the beam, I the inertia moment of the cross-section area, and the Young's modulus of the beam material.

To calculate the ith modal coordinate $\eta_i(t)$, the kinetic energy T and the potential energy P are expressed in terms of the beam deformation $w(x,t) = \sum_{i=1}^{n}\eta_i(t)\cdot\psi_i(x)$. The calculated kinetic and potential energies are then submitted into the Lagrange equation $\frac{d}{dt}\left(\frac{\partial T}{\partial\dot\eta_i}\right) - \frac{\partial T}{\partial\eta_i} - \frac{\partial V}{\partial\eta_i} = Q_i$ where Q_i is the generalized force for the ith mode. The ith modal coordinate equation can be given as

$$C_i\cdot\ddot\eta_i + \frac{EI}{\rho A}G_i\cdot\eta_i = -D_i\ddot\theta \tag{9}$$

where $C_i = \int_0^l\psi_i(x)^2\,dx$, $G_i = \int_0^l\left(\frac{d^2}{dx^2}\psi_i(x)\right)^2 dx$, and $D_i = \int_0^l\psi_i(x)\cdot x\,dx$.

Taking the Laplace transform of Eqn. (8), the deformation of the slewing beam can be written in the Laplace domain as

$$w(x,s) = \sum_{i=1}^{n} \eta_i(s) \cdot \psi_i(x) = -\theta(s) \sum_{i=1}^{n} \frac{\psi_i(x)D_i s^2}{C_i s^2 + \frac{EI}{\rho A}G_i} \tag{10}$$

Reorganizing Eqn. (10), the transfer function of the deformation of the slewing beam to the angular position is given as

$$G_{w\theta}(s) = \frac{w(x,s)}{\theta(s)} = -\sum_{i=1}^{n} \frac{\psi_i(x)D_i s^2}{C_i s^2 + \frac{EI}{\rho A}G_i} \tag{11}$$

In this work, the LPM model is also established to investigate the vibration properties of the slewing beam. In the LPM, the continuous beam is discretized using concentrated masses connected by massless springs. The developed LPM model is capable of taking into account the impact of motor rotor (plus hub) inertia and motor motion controller on the vibration properties of the slewing link. The boundary conditions used in the LPM model can be easily tuned to be close to the real boundary conditions which are between the pinned-free and the fixed free. The determination of the exact boundary condition of flexible-link robot manipulator is a complicated and challenging issue. Due to the limitation of the space, the detailed derivation of the LPM mode is not presented in this work but the simulations are conducted and given for dynamic analysis and comparison in Section 6.

5. Electrical-Mechanical System Model

Integrating the DC motor dynamics Eqn. (5) in Section 3 and the slewing beam dynamics Eqn. (11) in Section 4, the electrical-mechanical system model of the lightweight link robot manipulator can be presented using a block diagram as shown in Fig.4. The electrical-mechanical system dynamic model can be given in terms of a transfer function as

$$G_{wV}(s) = \frac{w(x,s)}{V_a(s)} = G_{w\theta}(s).G_{\theta V}(s) = -\frac{K_m}{L_a J s^3 + R_a J s^2 + (R_a b + K_m K_b)s} \cdot \sum_{i=1}^{n} \frac{\psi_i(x)D_i s^2}{C_i s^2 + \frac{EI}{\rho A}G_i} \tag{12}$$

Electrical-Mechanical System Model

$V_a(s)$ → Motor Dynamics $G_{\theta V}(s)$ in Eqn. (5) → $\theta(s)$ → Slewing Beam Dynamics $G_{w\theta}(s)$ in Eqn. (11) → $w(x,s)$
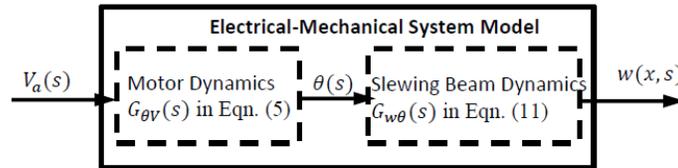
Fig. 4. Schematic diagram of the electrical-mechanical system model

Taking the inverse Laplace transform of Eqn. (12), the ordinary differential equation of the electrical-mechanical dynamics of a lightweight robot manipulator can be obtained. Although it is beyond the goal of this work, the obtained electrical-mechanical system dynamic model can be used to investigate: (1) how the DC dynamics and control impact the deformation of the flexible link; (2) how the vibration of the slewing link is suppressed by controlling the DC motor.

6. Numerical Simulation and Experimental Testing

In this section, numerical simulations and experimental testing are conducted, and then the numerical and experimental results are compared and analysed to validate the developed dynamic models. As shown in Fig. 5, an experimental system was developed using NI LabView real-time module and CompactRIO for real-time control of DC motor and vibration testing. The lightweight link is a beam made of aluminium with the geometrical parameters: length 0.395 m, width 0.0395 m, thickness 0.0014 m.
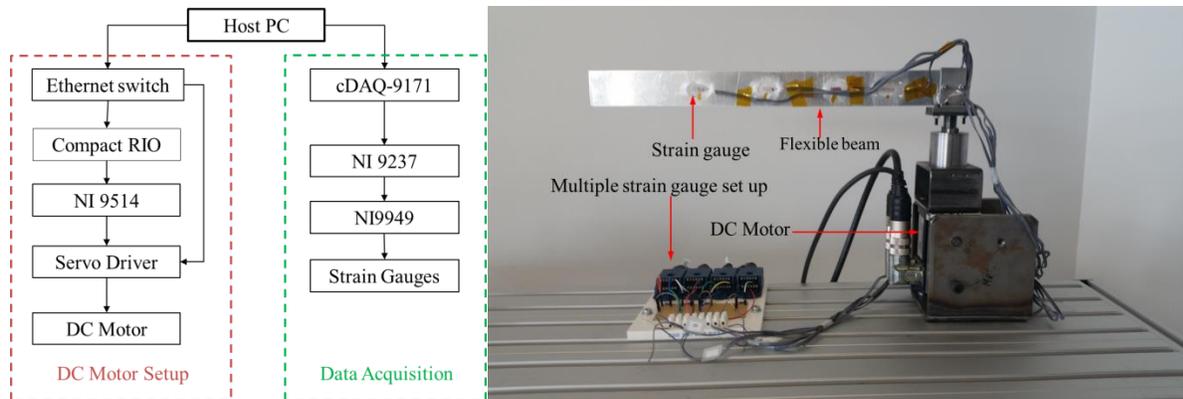
Fig. 5. Schematic diagram (left) and photo (right) of the experimental system setup

6. 1. Simulation and Testing of DC motor Dynamics

To verify the DC dynamic models, the DC motor shaft angular position and velocity are measured and recorded with the given input voltage or current (only the current can be directly measured for the current testing system as shown in Fig. 6). Experimental results are compared to the numerical results based on the analytical models developed in Section 2. As shown in Fig. 7, the comparison and analyses demonstrate the numerical simulation results well agree to the experimental results and the dynamics models developed in Section 2 are validated.
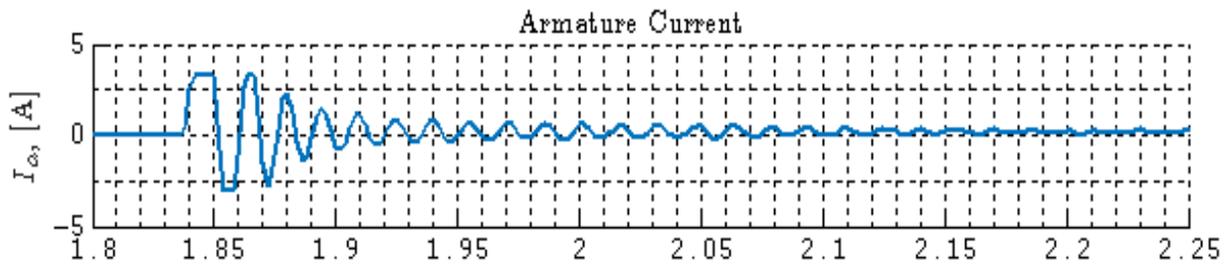
Fig. 6. Armature current of the DC dynamics
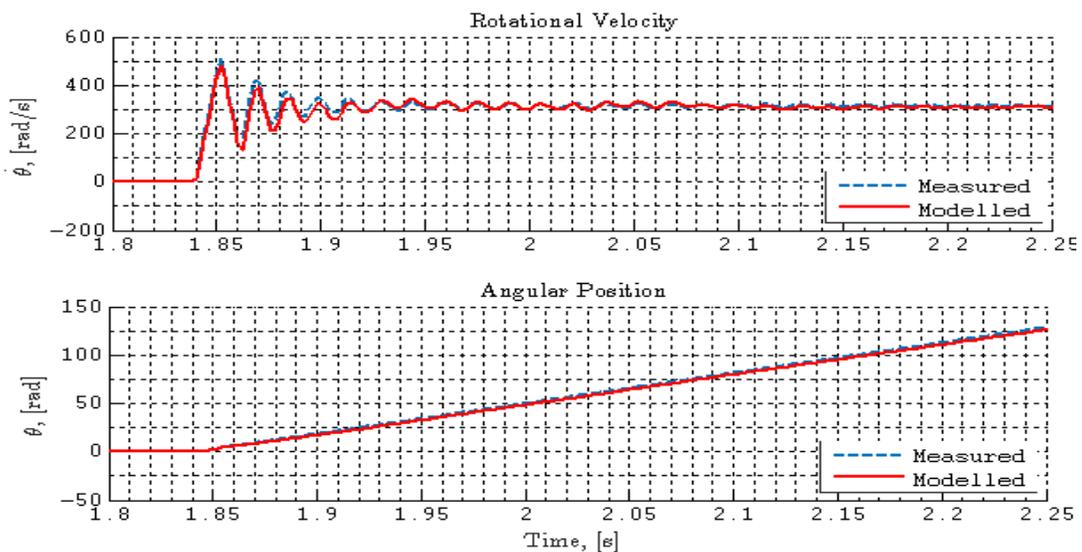
Fig. 7. Simulation and testing results of the DC angular positon and velocity

6. 2. Simulation and Testing on Modal Properties of the Flexible Beam

Table. 1. Frequency testing and simulation of the flexible beam

Frequency (Hz)	Fixed-Free (Cantilever)		Pinned-Free	Driven by Motor		
	Theoretical	Experimental	Theoretical	Experimental	LPM	AMM
1st mode	7.8	7.2	34	28	30	7.8
2nd mode	49	45	110	75	98	-
3rd mode	140	119	230	-	200	-

The modal properties are tested using an impact hammer. The hamper is used to hit the beam, and the strain gauges are used to pick up the vibration of the beam. The testing are conducted for two cases: the beam is clamped at one end, namely assuming the beam as a cantilever beam; the beam is held by the DC motor with the controller turning on for simulating the driving situation. The measured frequencies are listed in the Table 1. The theoretical frequencies are calculated for different cases and listed in the Table 1 as well. As shown Table 1, the boundary condition of the driven beam is between the fixed-free and pinned-free, and is very close to the boundary condition used in the LPM model as it is capable of including the impact of the hub and rotor on the vibration properties. The boundary condition could change with the system setup and DC motor controller design, and it is a complex issue. The detailed investigations on the variable boundary condition remain the focus of our ongoing research, and are not discussed in this work due to the limited space.

6. 3. Simulation and Testing of the Beam Driven by the DC Motor

The simulation and testing are conducted to a single flexible-link driven by the DC motor. The current applied to the armature is recorded as shown in the Fig. 8.
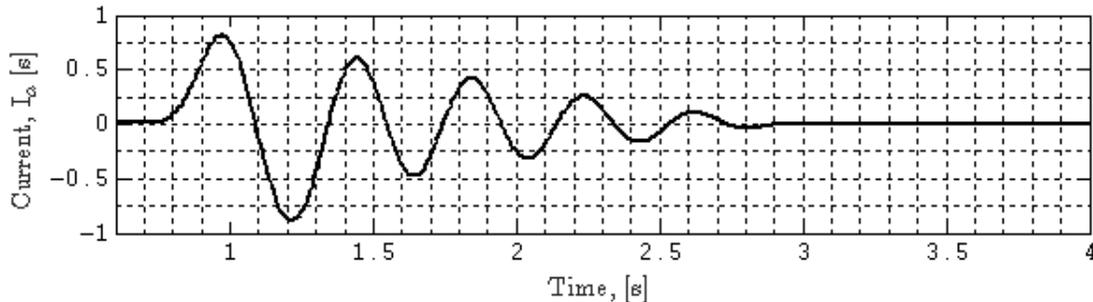
Fig. 8. Current applied to the armature of the DC motor

The shaft angle of the DC motor is acquired by the encoder and depicted as shown in Fig. 9. The tip deformation of the slewing beam is measured using the strain gauges. The comparison of tip deformation between the testing and simulations of LPM and AMM models are shown in Fig. 10. The comparison shows that the simulation results using the developed electrical-mechanical model agree well on the experimental results. The LPM-based model has better results as expected. The reason is that the LPM model employs the variable and adjustable boundary condition by including the impact of rotor inertia and motion controller on the structural vibration of the beam. This is the motivation of our ongoing work that will be devoted to the determination of the boundary condition in electrical-mechanical modelling and vibration characterization of flexible-link manipulators.

7. Conclusion and Discussion

The system dynamics of a lightweight-link robot manipulator has been investigated by including the DC motor dynamics. The electrical-mechanical dynamic model of the robot manipulator has been

established as the function of the voltage applied to the DC motor as the input, and the elastic deformation of the lightweight link as the output. To verify the developed system model, a real-time control and testing system was established using NI CompactRIO and LabView Real-time module so that the experimental testing was conducted to compare the numerical simulation results. The developed model provides the essential insights on how the DC motor dynamics and control impact the deformation of the driven flexible beam, and how the deformation of flexible links can be reduced by controlling the DC motor. The research in this work is targeted at a single link robot manipulator, but the methodology can be extended to a robot system with multiple links.
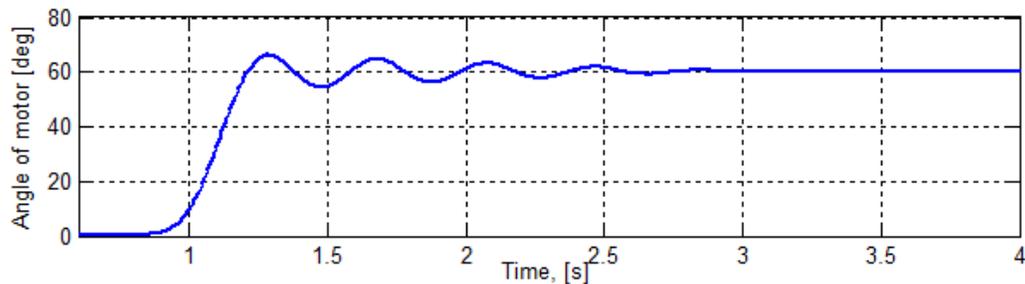
Fig. 9. Rotational angle of the DC motor
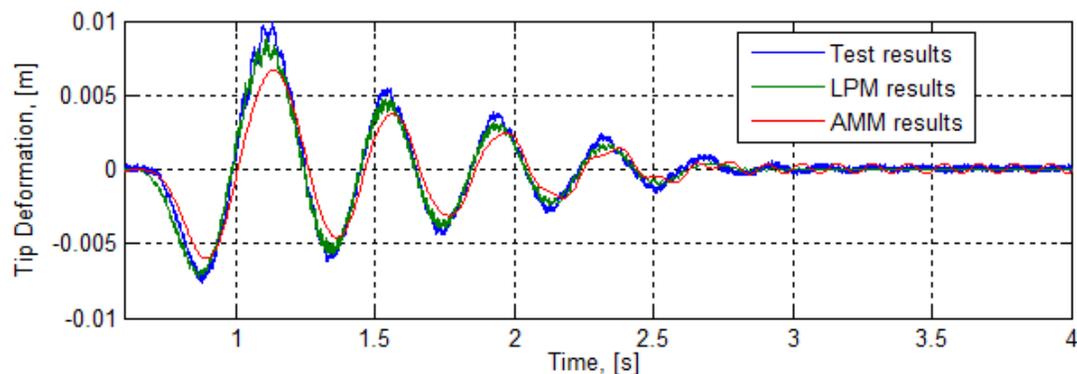
Fig. 10. Comparison of tip deformation between the testing and simulations

References

Asada, H., Ma, Z.-D., & Tokumaru, H. (1990). Inverse Dynamics of Flexible Robot Arms: Modeling and Computation for Trajectory Control. *ASME. J. Dynamic Sys. Meas. Control,* 112, 177-185.

Barieri, E., & Ozguner, U. (1988). Unconstrained and Constrained Mode Expansion for a Flexible Slewing Link. *ASME J. Dynamic Sys. Meas. Control,* 110, 416-421.

Baruh, H., & Tadikonda, K. (1989). Issues in the Dynamics and Control of Flexible Robot Manipulators. *AIAA J. Guidance Control Dynamics,* 12(5), 559-671.

Bellezza, F., Lanari, L., & Ulivi, G. (1990). Exact Modeling of the Flexible Slewing Link. *Proceedings of the IEEE International Conference on Robotics and Automation,* 734-739.

Benosman, M., & Vey, G. L. (2004). Control of Flexible Manipulators: A Survey. *Robotica,* 22, 533-545.

Book, W. (1993). Controlled Motion In An Elastic World. *ASME Journal of Dynamic Systems, Measurement, and Control,* 115, 252–260.

Book, W. J. (1984). Recursive Lagrangian Dynamics of Fexible Manipulator Arms. *Int. J. Robotics Res.,* 3(3), 87-101.

Cleghorn, W. L., Fenton, R. G., & Tabarrok, B. (1981). Finite Element Analysis of Hign-Speed Flexible Mechanisms. *Mech. Mach. Theory,* 16, 407-424.

Dwivedy, S. K., & Eberhard, P. (2006). Dynamic Analysis of Flexible Manipulators, a Literature Review. *Mechanism and Machine Theory,* 41, 749-777.

Erdman, A. G., Sandor, G. N., & Oakberg, R. G. (1972). A General Method for Kinetoelastodynamic Analysis and Sythesis of Mechanisms. *ASME J. Engng Ind.,* 94, 1193-1205.

Ge, S. S., Lee, T. H., & Zhu, G. (1997). A New Lumping Method of a Flexible Manipulator. *Proceedings of the American Control Conference, Albuquerque,* 1412-1416,

Hustings, G. G., & Book, W. J. (1986). Verification of a Linear Dynamic Model for Flexible Robotic Manipulators. *Proc. IEEE Int. Conf. Robot. Automation,* 1024-1029.

Imam, S. G. N., & Kraner, S. N. (1973). Deflection and Stress Analysis in High Speed Planar Mechanisms with Elastic Links. *ASME J. Engng Ind.,* 95, 541-584.

Low, K. H., & Lau, M. W. S. (1995). Experimental Investigation of the Boundary Condition of Slewing Beams Using A High-Speed Camera System. *Mechanism and Machine Theory,* 30, 629-643.

Lowen, G. G., & Jandrasits, W. G. (1972). Survey Of Investigations Into The Dynamic Behavior Of Mechanisms Containing Links With Distributed Mass And Elasticity. *Mechanism and Machine Theory,* 7, 3-17.

Lowen, G. G., & Chassapis, C. (1986). The Elastic Behavior of Linkage: An Update. *Mechanism and Machine Theory,* 21(1), 33-42.

Megahed, S. M., & Hamza, K. T. (2004). Modeling and Simulation of Planar Flexible Link Manipulators with Rigid Tip Connections to Revolute Joints. *Robotica,* 22, 285–300.

Dupac, M., & Noroozi, S. (2014). Dynamic Modeling and Simulation of a Rotating Single Link Flexible Robotic Manipulator Subject to Quick Stops. *Journal of Mechanical Engineering*, 60(7-8), 475-482.

Nath, P. K., & Ghosh, A. (1980). Kineto-Elastodynamic Analysis of Mechanisms by Finite Element Method. *Mech. Mach. Theory,* 15, 179-197.

Shabana, A.A. (1997). Flexible Multibody Dynamics: Review of Past and Recent Developments. *Multibody System Dynamics,* 1, 189– 222.

Shabana, A. A. (1996). Resonance Conditions and Deformable Body Co-Ordinate Systems. *Journal of Sound and Vibration,* 192, 389-398.

Tosunogle, S., Lin, S.-H., & Tesar, D. (1992). Accessibility Controllability of Flexible Robotic Manipulators. *ASME J. Dynamic Sys. Meas. Control,* 114, 50-58.

Turic, D. A., & Midha, A. (1984). Generalized Equations Of Motion For The Dynamic Analysis Of Elastic Mechanism Systems. *ASME J. Dyn. Sys. Meas. Control,* 106, 243-248.

Usoro, P. B., Nadira, R., & Mahil, S. S. (1986). A Finite Element/Lagrangian Approach to Modelling Lightweight Flexible Manipulators. *ASME Journal of Dynamic Systems, Measurements, and Control,* 108,198-205.

Zhang, X., & Yu, Y. (2009). A New Spatial Rotor Beam Element for Modeling Spatial Manipulators with Moint and Link Flexibility. *Mechanism and Machine Theory,* 35(3), 403-42.

Zhang, X., Mills, J. K., & Cleghorn, W. L. (2007). Dynamic Modeling and Experimental Validation of a 3-PRR Parallel Manipulator with Flexible Intermediate Link. *Journal of Intelligent and Robotic Systems,* 50(4), 323-340.